transfer phenomenon is reported by Sherman et al.[4] in a numerical study of laminar parallel slot injection wherein it is found that, for the same coolant flow, increasing slot height provides more effective cooling than increasing jet velocity. As expected, the boundary-layer thickening and insulating effect observed in parallel slot injection is more pronounced than that reported here for oblique injection. However, the parallel slot configuration is not suitable for engineering applications such as turbine blade cooling.

2) As indicated in Fig. 1, well downstream of the slot, the cooling effectiveness of tangential injection is nearly equal to that of normal injection. Thus, if only moderate effectiveness, say 0.3, is required, it is preferable to use tangential injection, which not only serves the purpose of film cooling but also increases aerodynamic performance. In general, a compromise must be considered in film cooling design.

3) As indicated in Fig. 2, where coolant mass flow is held fixed, a low injection velocity with a wide slot is preferable to a high velocity with a narrow slot. Although the effect is small for normal injection, it is more pronounced for tangential injection.

4) As indicated in Fig. 3, the larger the boundary-layer thickness upstream of the slot, the greater the effectiveness, particularly near the slot region. However, this influence diminishes as the injection angle α is decreased.

5) As indicated in Fig. 3, the presence of an upstream slot increases cooling effectiveness. However, the degree of influence is strongly dependent on the spacing between slots, since the increased efficiency is primarily attributed to the reduction of temperature in the boundary layer, with increase of boundary-layer thickness being a secondary consideration.

References

[1] Goldstein, R. J., "Film Cooling," *Advances in Heat Transfer*, Vol. 7, 1971, pp. 321–379.

[2] Nilson, R. H. and Tsuei, Y. G., "A Numerical Method for Boundary Layer Equations," Report, Jan. 1974, Dept. of Mechanical Engineering, Univ. of Cincinnati, Cincinnati, Ohio.

[3] Patankar, S. V. and Spalding, D. B., "A Finite Difference Procedure for Solution of the Equations of the Two Dimensional Boundary Layer," *International Journal of Heat and Mass Transfer*, Vol. 10, No. 10, 1967, pp. 1389–1412.

[4] Sherman, A., Yeh, H., McAssey, E., and Reshotko, E., "Multiple Slot Laminar Film Cooling," *AIAA Journal*, Vol. 11, No. 10, Oct. 1973, pp. 1413–1414.

Combined Effects of Nose Bluntness and Cone Angle on Unsteady Aerodynamics

L. E. ERICSSON,* R. A. GUENTHER,† W. R. STAKE,† AND G. S. OLMSTED†

Lockheed Missiles and Space Company, Inc., Sunnyvale, Calif.

NOSE bluntness effects play an important role in aerodynamics of slender bodies in hypersonic flow. When trying to use experimental data for blunted slender cones one encounters the problem that more than one of the geometric parameters, e.g., cone frustum angle and nose bluntness, have

Received November 12, 1973; revision received January 10, 1974.

Index categories: Entry Vehicle Dynamics and Control; Nonsteady Aerodynamics; Supersonic and Hypersonic Flow.

* Consulting Engineer. Associate Fellow AIAA.

† Aerodynamics Engineer, Senior.

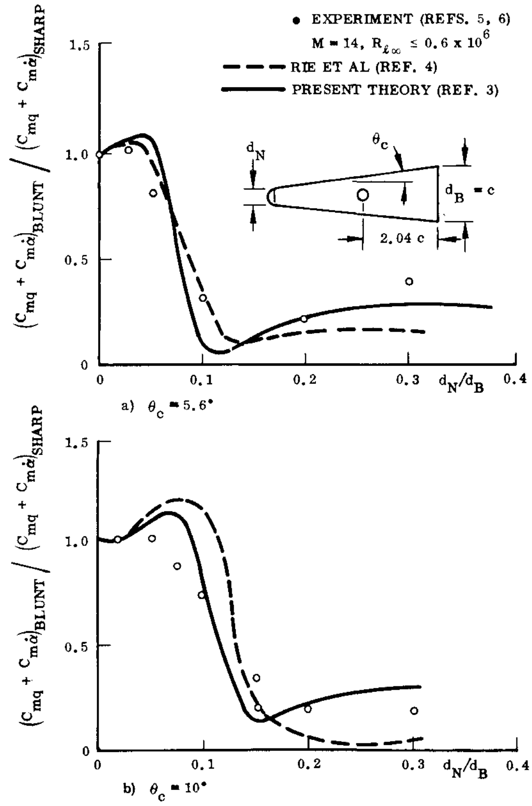

Fig. 1 Comparison between predicted and measured effect of nose bluntness on slender cone damping at $\alpha = 0$.

been changed between tests. Cone angles of 5°–20° have been used in combinations with nose bluntnesses from zero to $(d_N/d_B) = 0.50$. If through the selection of suitable scaling para-

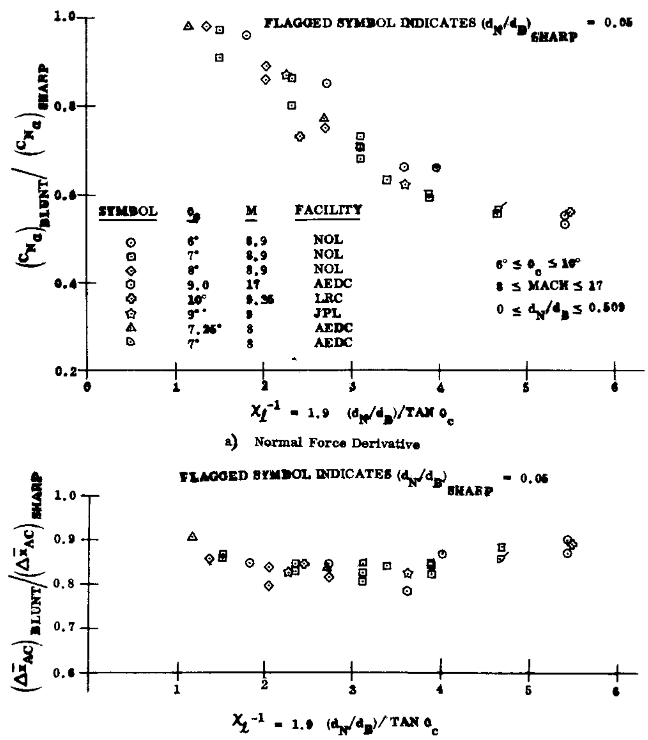

Fig. 2 Scaling of experimental static data for slender blunted cones.

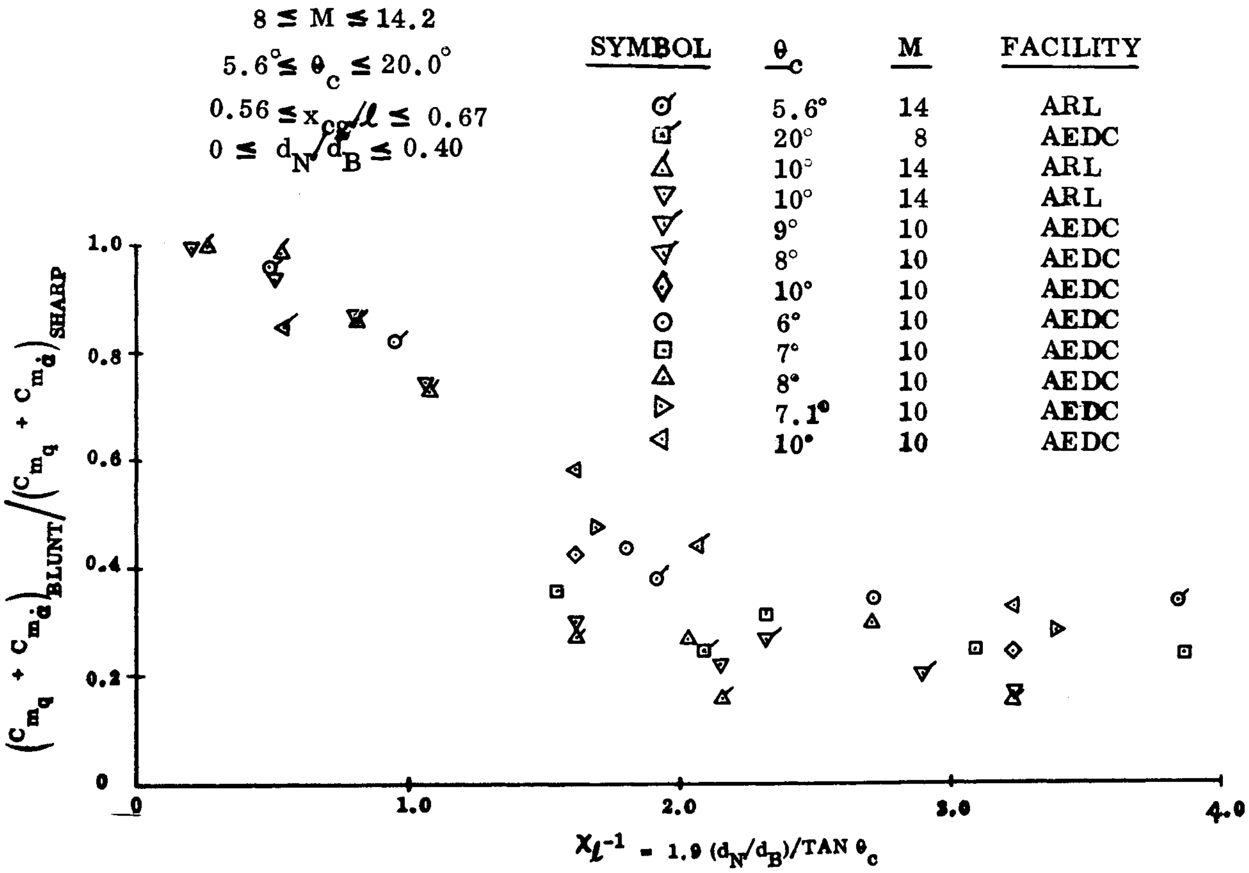

a) Experimental Data

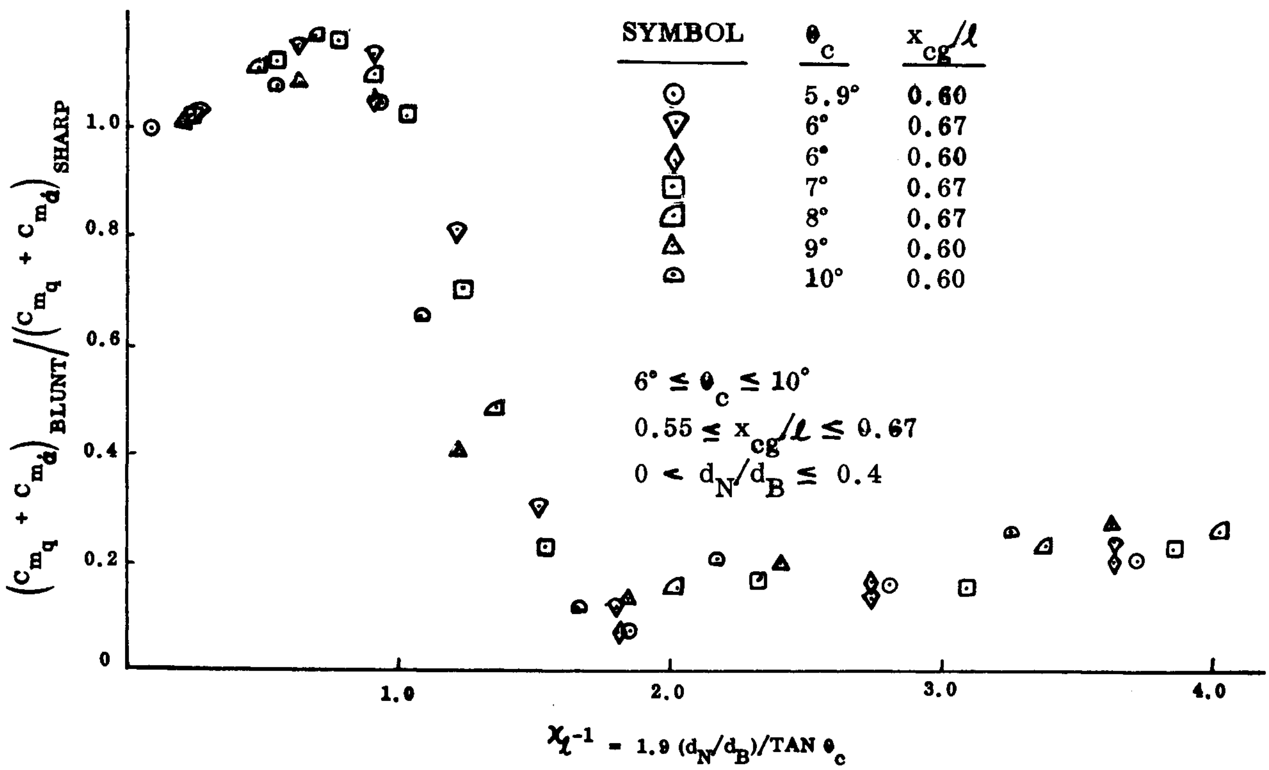

b) Theoretical Damping Derivative

Fig. 3 Scaling of damping derivatives for slender blunted cones.

meters all these separate pieces of valuable experimental data could be used to define the combined effects of nose bluntness and cone angle, the hypersonic vehicle designer obviously would stand to gain a great deal. The present Note shows how a developed unsteady embedded Newtonian theory[1-3] indeed provides such scaling parameters.

The simple analytic theory[3] provides data that agree well with a more "exact" and time-consuming numerical method,[4] and both methods predict the experimentally measured unsteady aerodynamic characteristics[5,6] (Fig. 1). By measuring the nose bluntness effect as the fractional change from sharp cone characteristics, the inviscid theoretical results can be compared with viscous experimental data. Viscous interaction[7,8] and sting interference[5,9,10] effects that are common to both blunted and sharp cones are eliminated in this manner. Nose bluntness should have a negligible effect on the viscous crossflow of a thin turbulent boundary layer, and the effect is probably small also for a purely laminar boundary layer, i.e., as long as boundary-layer transition does not occur on the (aft) body.[11,12] There is a question mark in regard to the sting interference effects, as there is experimental evidence indicating that nose bluntness can have a significant effect on the near wake flow[13] and, therefore, on the sting interference.[10] However, Walchner and Clay made sure that their experimental results were not affected by sting interference.[5,6,9] Thus, the comparison made in Fig. 1 should be valid.

The embedded Newtonian theory provides the following scaling parameter for the combined effects of nose bluntness (d_N/d_B) and cone (half) angle (θ_c):

$$\chi_l = \frac{\tan\theta_c}{d_N/d_B}\Big/ 2C_{DN}{}^{1/2}$$

that is, slender‡ cones with spherical nose bluntness, $C_{DN} = 0.9$, have the same "percentage" change from sharp cone characteristics as long as the ratio between cone angle (θ_c) and nose bluntness (d_N/d_B) is the same. This is true for both inviscid theoretical data and viscous experimental data.[2] The only requirement is that the center of gravity (x_{CG}) is the same based on sharp cone length (l), i.e., $x_{CG}/l = \text{const}$. However, for a realistic center of gravity, $0.30 \leqq \Delta\bar{x}/l \leqq 0.40$ or $0.70 \geqq x_{CG}/l \geqq 0.60$, the dynamic derivative varies rather slowly with x_{CG}/l (see Fig. 8 of Ref. 2). It is undoubtedly true that the experimental scatter of the measured damping derivative usually is as large as or larger than changes due to *CG*-variations. This makes it possible to correlate *all* blunted cone data regardless of *CG*-location in the following manner:

$$(C_{N_\alpha})_{\text{BLUNT}}/(C_{N_\alpha})_{\text{SHARP}},\ (\Delta\bar{x}_{AC})_{\text{BLUNT}}/(\Delta\bar{x}_{AC})_{\text{SHARP}},\ (C_{m_q}+C_{m_{\dot{\alpha}}})_{\text{BLUNT}}/(C_{m_q}+C_{m_{\dot{\alpha}}})_{\text{SHARP}}$$

can be plotted vs $\chi_l^{-1} = 1.9(d_N/d_B)/\tan\theta_c$ to correlate all experimental data. Figure 2 and Fig. 3a show that all the available experimental data, when represented in this form, does indeed collapse to provide the practicing engineer with one preliminary design curve for the combined effects of nose bluntness and cone angle. (Any possible sting interference effects[10] are "buried" in the data scatter.)

Because of viscous interaction, the Reynolds number has a significant effect on the experimental data. This accounts for some of the scatter in Figs. 2 and 3. When comparing inviscid theory with correlated experimental data, the viscous interaction effect becomes very apparent[2] (compare Figs. 3a and 3b). The viscous interaction displaces the bow shock and produces an apparent increase of the nose bluntness of the tested cone models, thus shifting the experimental curve to higher χ_l^{-1} for small to moderate magnitude nose bluntness and preventing it from reaching down to the sharp cone value at $\chi_l^{-1} = 0$. For large nose bluntness it is not the induced bow shock curvature but rather the local negative load due to viscous interaction[21] that is the dominant effect.

‡ $\tan\theta_c \approx \theta_c$.

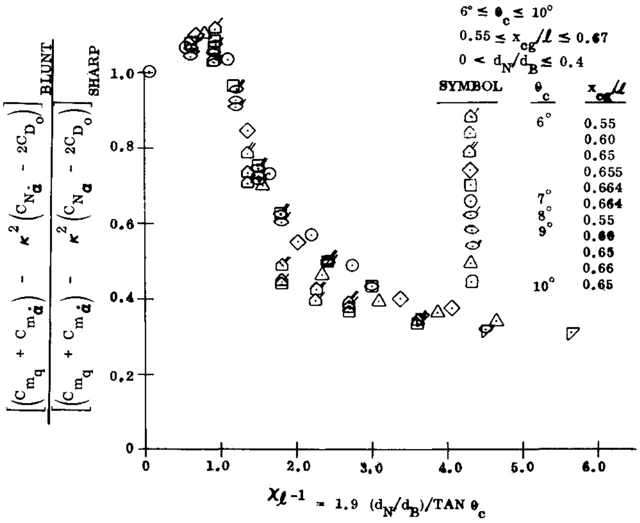

Fig. 4 Inviscid dynamic stability parameter of slender blunted cones in planar motion.

For a re-entry vehicle in planar motion, it can be shown that the dynamic stability criterion for a slender vehicle can be written as follows[22]:

$$(C_{m_q}+C_{m_{\dot{\alpha}}}) - \kappa^2(C_{N_\alpha} - 2C_{D_o}) < 0$$

The presented scaling laws also permit this additional dynamic stability parameter to be evaluated against the combined effects of nose bluntness and cone angle. Figure 4 shows the inviscid results given by unsteady embedded Newtonian theory.[3,23] The parameter is shown for $\kappa^2 = 1$, a typical value for slender re-entry bodies. The presented results suggest strongly that the missile designer can safely trade some of the standard nose bluntness-cone angle runs for tests giving information about the less known effects of nose asymmetry, damaged body, etc.

References

[1] Ericsson, L. E., "Unsteady Aerodynamics of an Ablating Flared Body of Revolution Including Effects of Entropy Gradient," *AIAA Journal*, Vol. 6, No. 12, Dec. 1968, pp. 2395–2401.

[2] Ericsson, L. E., "Universal Scaling Laws for Hypersonic Nose Bluntness Effects," *AIAA Journal*, Vol. 7, No. 12, Dec. 1969, pp. 2222–2227.

[3] Ericsson, L. E., "Effect of Nose Bluntness, Angle of Attack, and Oscillation Amplitude on Hypersonic Unsteady Aerodynamics of Slender Cones," *AIAA Journal*, Vol. 9, No. 2, Feb. 1971, pp. 297–304.

[4] Rie, H., Linkievicz, E. A., and Bosworth, F. D., "Hypersonic Dynamic Stability, Part III, Unsteady Flow Field Program," FDL-TDR-64-149, Pt. III, Jan. 1967, Flight Dynamics Lab., Wright-Patterson Air Force Base, Ohio.

[5] Walchner, O. and Clay, T., "Nose Bluntness Effects on the Stability Derivatives of Cones in Hypersonic Flow," *Transactions of the 2nd Technical Workshop on Dynamic Stability Testing*, Vol. 1, Paper 8, Arnold Engineering Development Center, Arnold Air Force Station, Tenn., April 20–22, 1965.

[6] Clay, J. T., "Nose Bluntness, Cone Angle, and Mach Number Effects on the Stability Derivatives of Slender Cones," ARL 67-0185, Sept. 1967, Aerospace Research Lab., Wright-Patterson Air Force Base, Ohio.

[7] Orlik-Rückemann, K. J., "Dynamic Viscous Pressure Interaction in Hypersonic Flow," Aero. Rept. LR-535, July 1970, National Research Council, Ottawa, Canada.

[8] Ericsson, L. E. and Reding, J. P., "Ablation Effects on Vehicle Dynamics," *Journal of Spacecraft and Rockets*, Vol. 3, No. 10, Oct. 1966, pp. 1476–1483.

[9] Walchner, O., private communication of unpublished data on hypersonic dynamic support interference, March 22, 1972, Aerospace Research Lab., Wright-Patterson Air Force Base, Ohio.

[10] Reding, J. P. and Ericsson, L. E., "Dynamic Support Interference," *Journal of Spacecraft and Rockets*, Vol. 9, No. 7, May 1972, pp. 547–553.

[11] Ericsson, L. E., "Effect of Boundary-Layer Transition on Vehicle Dynamics," *Journal of Spacecraft and Rockets*, Vol. 6, No. 12, Dec. 1969, pp. 1404–1409.

[12] Ericcson, L. E., "Transition Effects on Slender Vehicle Stability and Trim Characteristics," *Journal of Spacecraft and Rockets*, Vol. 11, No. 1, Jan. 1974, pp. 3–11.

[13] Peterson, C. W. and Bogdonoff, S. M., "An Experimental Study of Laminar Hypersonic Blunt Cone Wakes," AIAA Paper 69-714, San Francisco, Calif., 1969.

[14] Ward, L. K. and Uselton, B. L., "Dynamic Stability Results for Sharp and Blunted 10° Cones at Hypersonic Speeds," *Transactions of the 3rd Technical Workshop on Dynamic Stability Problems*, Vol. III, Paper 2, NASA Ames Research Center, Moffett Field, Calif., Nov. 4–7, 1968.

[15] Harris, J. E., "Force-Coefficient and Moment-Coefficient Correlations and Air-Helium Simulation for Spherically Blunted Cones," TN D-2184, Nov. 1965, NASA.

[16] Technical Staff, "Experimental Investigation of the Aerodynamic Characteristics of 9 Degree Half-Angle Cones and Varying Degrees of Bluntness at Mach Number 9," Publication U-1638, April 1962, Aeronutronics, Newport Beach, Calif.

[17] Martellucci, A., Neff, R. S., and Rittenhouse, C., "Mass Addition Effects on Vehicle Forces and Moments—Comparison Between Theory and Experiment," Document 69 SD934, SAMSO TR 69-384, Sept. 1969, Space and Missiles System Organization, U.S. Air Force.

[18] Burt, G. E., "Effects of Nose Bluntness and Base Shape on the Dynamic Stability Characteristics of Ablating and Non-Ablating 8-Degree Cones at Mach 10," AEDC-TR-66-31, Feb. 1966, Arnold Engineering Development Center, Tullahoma, Tenn.

[19] Hobbs, R. B., "Hypersonic Dynamic Stability," FDL-TDR-64-149, Pt. 2, Jan. 1967, Flight Dynamics Lab., Wright-Patterson Air Force Base, Ohio.

[20] Ward, L. K. and Uselton, B. L., "Dynamic Stability Tests of Three Re-entry Configurations at Mach 8," AEDC-TDR-62-11, Jan. 1962, Arnold Engineering Development Center, Tullahoma, Tenn.

[21] Friberg, E. G. and Walchner, O., "Pressure Correlation for Blunted Slender Cones," *AIAA Journal*, Vol. 7, No. 8, Aug. 1969, pp. 1618, 1619.

[22] Nelson, R. L., "Measurement of Aerodynamic Characteristics of Re-Entry Configurations in Free Flight at Hypersonic and Near-Orbital Speeds," AGARD Rept. 380, July 1961.

[23] Ericsson, L. E., "Unsteady Embedded Newtonian Flow," *Astronautica Acta*, Vol. 18, No. 5, Nov. 1973, pp. 309–330.

Calculation of Laminar Boundary Layers on Continuous Surfaces by Meksyn's Method

A. V. MURTHY* AND K. S. HEBBAR†
National Aeronautical Laboratory, Bangalore, India

IN the case of laminar boundary layers on continuous surfaces, Eickhoff[1,2] has shown that the linearization of the boundary-layer equations leads to analytical results for the heat-transfer rates that agree well with the numerical results of Rhodes and Kaminer[3] over a wide range of Prandtl numbers ($0.1 \leq \sigma \leq 1000$). In general, this method can also be applied for the analysis of the shock tube boundary layers. In fact, this was done some years ago by the authors[4,5] and the results obtained were compared with the numerical results of Mirels.[6] The purpose of this Note is to present some important results obtained by the authors. It may be noted that these results agree with those of Eickhoff when the shock strength $\lambda \gg 1$; they can also be used for values of λ relevant to shock tube boundary layers ($1 \leq \lambda \leq 6$ for $\gamma = 1.4$).

Following Mirels and the usual notation, the governing equations and the boundary conditions for solving the laminar boundary layer which develops on an uninsulated wall behind a shock wave advancing into a stationary fluid are

$$f''' + ff'' = 0 \tag{1}$$

$$s'' + \sigma f s' = 0 \tag{2}$$

$$f(o) = 0, \quad f'(o) = \lambda, \quad f'(\infty) = 1 \tag{3}$$

$$s(o) = 1, \quad s(\infty) = 0 \tag{4}$$

Using Meksyn's technique,[7] Eqs. (1–4) can be solved[4] for the two unknowns $f''(o)$ and $s'(o)$—the two important wall derivatives the former relating to wall shear and the latter to wall heat transfer. By integrating Eqs. (1) and (2) from zero to infinity and then substituting the boundary conditions (3) and (4), we get

$$1 - \lambda = \alpha \int_0^\infty e^{-F}\, d\eta \tag{5}$$

and

$$-1 = k \int_0^\infty e^{-\sigma F}\, d\eta \tag{6}$$

where

$$\alpha = f''(o), \quad k = s'(o) \quad \text{and} \quad F = \int_0^\eta f\, d\eta$$

For $\eta \to 0$, the series expansion for F is

$$F = \frac{\lambda\eta^2}{2!} + \frac{\alpha\eta^3}{3!} - \frac{\alpha\lambda\eta^5}{5!} + \cdots \tag{7}$$

and by inversion,

$$\eta = A_0 F^{1/2} + (A_1/2)F + (A_2/3)F^{3/2} + \cdots \tag{8}$$

where $A_0 = (2/\lambda)^{1/2}$, $A_1 = -(2\alpha/3\lambda^2)$, $A_2 = (5/6)(\alpha/\lambda^2)^2(\lambda/2)^{1/2}$, etc. After integrating Eqs. (5) and (6) using Eq. (8), we get

$$1 - \lambda = \alpha(B_0 + B_1\alpha + B_2\alpha^2 + \cdots) \tag{9}$$

and

$$-1 = k\left(\frac{B_0}{\sigma^{1/2}} + \frac{B_1}{\sigma}\alpha + \frac{B_2}{\sigma^{3/2}}\alpha^2 + \cdots\right) \tag{10}$$

where $B_0 = (\pi/2\lambda)^{1/2}$, $B_1 = -(1/3\lambda^2)$, $B_2 = (5/24)(1/\lambda^4)(\pi\lambda/2)^{1/2}$; etc., α and k may be evaluated from Eqs. (9) and (10), respectively. Hsu[8] also has obtained the value of α using Meksyn's technique and he gives a more general form of Eq. (9) by retaining higher order terms in the series expansion (7). However, even the first three terms on the RHS of Eq. (9) provide a good approximation and α can be calculated by solving the cubic equation

$$\alpha^3 + p\alpha^2 + q\alpha + r = 0 \tag{11}$$

where

$$p = -\frac{8}{5}\left(\frac{2}{\pi}\right)^{1/2}\lambda^{3/2}, \quad q = \frac{24}{5}\lambda^3, \quad r = \frac{24}{5}\left(\frac{2}{\pi}\right)^{1/2}\lambda^{7/2}(\lambda - 1)$$

It may be easily verified that there is only one real root of α which is of interest to the present problem and the other two are complex. If only the first two terms in the series (8) are retained, the resulting equation for α is a quadratic and the solution is obtained in a closed form as

$$\alpha = \left(\frac{9\pi}{8}\right)^{1/2}\lambda^{3/2}\left[1 - \left\{\frac{8+3\pi}{3\pi} - \frac{8}{3\pi\lambda}\right\}^{1/2}\right] \tag{12}$$

Once α is known, k can be easily determined from Eq. (10). Taking only the first three terms on the RHS of Eq. (10), we get

$$k = \frac{-\sigma^{1/2}}{\left(\dfrac{\pi}{2\lambda}\right)^{1/2} - \dfrac{\alpha}{3\lambda^2\sigma^{1/2}} + \left(\dfrac{5}{24}\right)\left(\dfrac{\alpha}{\lambda^2}\right)^2\left(\dfrac{1}{\sigma}\right)\left(\dfrac{\pi\lambda}{2}\right)^{1/2}} \tag{13}$$

Received November 26, 1973. The authors wish to acknowledge R. Narasimha for his suggestions and discussions during the course of the work reported herein.

Index category: Boundary Layers and Convective Heat Transfer—Laminar.

* Scientist, Aerodynamics Division.

† Scientist, Aerodynamics Division; presently Research Assistant, Department of Aerospace Engineering, University of Maryland, College Park, Md.